RESEARCH ARTICLE

Distributed Secondary Control for Islanded Microgrids Considering Communication Delays

XINGHUA HUANG[1,2], YUANLIANG FAN[1,2], HAN WU[1,2], GONGLIN ZHANG[3], ZILI YIN[3], MUHAMMAD YASIR ALI KHAN [4], HAOMING LIU [4], (Senior Member, IEEE), AND JINGJING ZHAI[5]

[1]State Grid Fujian Electric Power Research Institute, Fuzhou 350007, China
[2]Fujian Key Enterprise Laboratory of High Reliability for Power Distribution Technology, Fuzhou 350003, China
[3]State Grid Fujian Electric Power Company Ltd., Fuzhou 350003, China
[4]School of Electrical and Power Engineering, Hohai University, Nanjing 211100, China
[5]School of Electric Power Engineering, Nanjing Institute of Technology, Nanjing 211167, China

Corresponding author: Jingjing Zhai (azhaijj@126.com)

ABSTRACT A distributed control of a Microgrid (MG) depends on the communication network for the exchange of information among the Distributed Generators (DGs). Most of the control schemes consider ideal communication among the DGs; however, in practical systems, delays are inherited in a system that can affect the dynamic performance and even destabilize an MG. Therefore, in this research work, a distributed Secondary Controller (SC) for an islanded MG is designed considering Communication Time Delays (CTDs). Sufficient delay-independent conditions for the robust stability of a buffer-free distributed averaging proportional integral control scheme are proposed. The CTDs are analyzed using the Lyapunov Krasovskii approach. A proposed method synchronizes the frequencies and voltages of the DGs to their respective references while confirming proportionate power sharing in the presence of CTDs. Moreover, different adaptive controllers are designed to update the fixed SC gain parameters to enhance the system's performance. Finally, the efficacy of the controller is demonstrated through simulation studies that validate its performance against load variation and plug-and-play functionality.

INDEX TERMS Communication delays, distributed control, hierarchical control, microgrid, secondary control.

I. INTRODUCTION

Microgrids have gained significant interest in the past decade due to their prosumer-friendly architecture, Renewable Energy Resources (RES) integration, and scalable nature. However, compared to conventional power systems, MGs have intermittent power generation due to RES (i.e., PV, wind, etc.) and have lower inertia. As a result, numerous issues arise, such as frequency deviation, system instability, voltage fluctuations, supply-demand imbalances, etc. [1].

The associate editor coordinating the review of this manuscript and approving it for publication was Shanying Zhu.

Due to these uncertainties, an MG is operated under highly stressed conditions; thus, a robust control strategy is required to guarantee an efficient and reliable operation [2].

Generally, a hierarchical structure is used to control an MG that consists of three levels. A basic or first level of hierarchy is a primary control that has a minimum decision time step and is concerned with MG stability. At a primary level, generally, a droop controller is used to regulate the frequency and voltage, ensuring appropriate power sharing, enabling Plug-and-Play (PnP) functionality, and enhancing system redundancy [3]. Although MG stability is achieved at the primary level however it pushes the frequencies and

voltages of the DGs away from their references. Hence, these deviations call for the next level of the hierarchical structure, i.e., a SC level. A key objective of an SC is to eliminate the aforementioned deviations in voltages and frequencies. Moreover, recently, more control objectives such as harmonic compensation, grid synchronization, power-sharing, etc. were introduced at the SC level [4]. Finally, the last level of hierarchy is a tertiary level that is concerned with economic optimization depending on energy prices and current markets [5]. This manuscript is mainly focused on the SC of an MG concerning CTDs; therefore, a tertiary level is not in the scope of this work.

A hierarchical control structure is implemented in three ways, i.e., distributed, decentralized, and centralized. However, due to the increased complexities of network dynamics, compared to other structures, a distributed structure is more attractive due to (a) low cost of cyber-network, (b) PnP operation, (c) requirement of a low bandwidth cyber-network, and (d) high robustness against failure of a single point [6]. As in a distributed control architecture, the information exchange among the DGs is performed through a communication network. However, during the information exchange, one of the major constraints that affect the system's stability and dynamic performance is the CTDs. The CTDs are intrinsic in a system and are generally instigated by network traffic or limited network bandwidth. Thus, a DG in an MG receives delayed information from their references and neighbouring DGs that can degrade the controller's performance, leading to system instability [7]. Therefore, it is very important to investigate the effect of CTDs on MG stability.

To cope with the CTDs, numerous researchers have recently developed different control strategies. For instance, the authors in [8] and [9] study the effect of fixed delays on the performance of the SC scheme. Similarly, in [10], a stochastic consensus based cooperative controller is presented for voltage and frequency regulation under noise disturbance and CTDs. These studies [8], [9], [10] considered that all the cyber-links have uniform delays; however, in practice, the delays are arbitrary rather than fixed. Hence, to cope with this limitation, the authors in [11] and [12] use a master-slave distributed SC scheme to develop the stability conditions for CTDs along with switching topology. However, this master-slave architecture introduces the additional uncertainty that the failure of a leader may lead to the instability of the system [13]. Similarly, the authors in [14] proposed a distributed finite-time control schemes for frequency regulation and optimal power sharing with CTDs by adjusting graph gains. This method is only feasible for small delays and requires optimizing the communication topology in advance. Moreover, in this research, multiple leaders are considered, which may lead to computational complexity.

The authors in [15] proposed a model predictive based distributed SC for the regulation of secondary frequency in the presence of CTDs. It improves the performance of the system and enhances the consensus convergence rate of the

islanded MG. However, it lacks discussion of the design of voltage regulation and reactive power sharing. A fuzzy logic based distributed cooperative SC to cope with the voltage deviation inherent in the droop controller is proposed in [16]. In this method, a fuzzy logic based SC controller is designed to optimize the SC gain coefficients to improve the quality of voltage waveforms in the presence of CTDs. However, a fuzzy controller requires extracting the fuzzy features manually, which makes it less flexible and robust for various disturbances [17].

In [18], the authors proposed a resilient H∞ theory based control structure for islanded MG, where the main emphasis is given to the upper bound of the time delay while no discussion is provided regarding the enhancement of time delay margin. The authors in [19] proposed a weight average prediction based distributed controller to mitigate the CTDs in an islanded MG. CTDs are studied using Lyapunov-Krasovskii function and linear matrix inequalities. Moreover, in this method, a time delay margin is enhanced, but the performance of the controller is degraded in case of multiple time delays. To mitigate the multiple time delays in an MG, a two layer distributed control architecture was developed [20]. Although this controller architecture mitigates the problem of multiple time delays, but due to the two layered structure, it might increase the implementation complexity. Moreover, this controller is designed considering DC networked MG; its validation in AC networked MG may require further enhancements.

The authors in [21] proposed an event triggered control law based distributed SC considering communication delays. In this method, it is assumed that all the DGs have the same fixed delays; however, this assumption is not valid in practical systems, as in large MGs, the DGs are located far from each other. Moreover, this controller only mitigates the delays in voltage, while no information is provided regarding the mitigation of CTDs in the frequency controller. Another consensus-based delay tolerant distributed control scheme is presented in [22]. However, the author is more tilted towards equal power sharing and tracking of varying averaging loads with finite time convergence. Moreover, in this method, all the DGs are assumed to have the same CTDs, which is practically not very feasible. Furthermore, the authors did not present the mathematical concept that validates the stability of the system in the presence of communication delays. To overcome the drawback of same CTDs in all the DGs another event trigger mechanism based distributed SC is presented in [23]. In this method, to ensure the stability of the system, a Lyapunov function is used to analyze the trigger conditions. Although this method performs very effectively and a theoretical derivation of stability is also provided but it lacks the explanation of the design of the controller parameters that is required to be studied further. The authors in [24] proposed a distributed SC based event driven mechanism with non-uniform delays. In this method, although the communication burden on the system is greatly

**TABLE 1.** Comparative analysis of proposed method with other methods.

REF	ASCGP	PNP	APF	FD	VD	BU	DD
[8]	×	×	NG	√	×	×	√
[9]	×	√	√	√	×	√	×
[11]	×	√	√	√	√	√	×
[14]	×	√	√	√	√	√	×
[15]	×	×	NG	√	×	×	×
[16]	√	√	√	√	×	×	×
[18]	×	√	√	√	√	√	√
[19]	×	×	√	√	√	√	×
[22]	×	√	√	√	×	√	√
[23]	×	√	√	√	√	√	×
P	√	√	√	√	√	×	×

Abbreviations: √: Presence of Feature, ×: Absence of Feature, ASCGP: Adaptive Secondary Control Gain Parameters, APF: Appropriate Power Flow, DD: Delay Dependent, FD: Fixed Delays, VD: Variable Delays, BU: Buffer Used, P: Proposed, H: High, M: Medium, NG: Not Given.

reduced but the authors did not present the stability of the system.

Although numerous state-of-the-art works discussed above presented a distributed SC scheme of an islanded MG that regulates the voltage and frequency and ensures accurate power sharing in the presence of CTDs. However, there are some limitations in these works, i.e., some of the control schemes consider small fixed CTDs, some consider a uniform CTDs in all DGs, some control schemes are delay-dependent having a limitation of upper bound of delay limits. Hence, to cope with these limitations in this research work a delay independent Distributed Averaging Proportional Integral (DAPI) based SC scheme is proposed. A comparative analysis of the proposed controller with the other most similar controllers discussed above are presented in Table 1. The principle contributions of this research work are presented below as follows:

- Different from [8], [9], [10], [21], and [22] that consider same CTDs for all DGs, in a proposed work, a distributed controller is designed that consider different small and large CTDs for all DGs;
- The distributed controllers presented in [12], [14], [18], [19], [23], [24], [25], and [26] are delay-dependent, i.e., have an upper bound for the delays in the communication channels. These methods require a compensation scheme (usually buffers) to minimize the deviations. The buffer-based control schemes require more power, storage, and computation to operate, which is not desirable. Moreover, the buffer memory may become insufficient if the systems scale up or the number of participants increases [27]. Therefore, using a buffer-based controller to minimize the time delay uncertainties may not be feasible. Hence, our proposed method avoids the use of any buffer based compensation scheme that greatly simplifies its implementation;
- In most of the existing distributed SCs, the dynamic adjustment of the SC control coefficients is not well explored. In this work, adaptive controllers are designed that update the SC gain parameters at every sampling
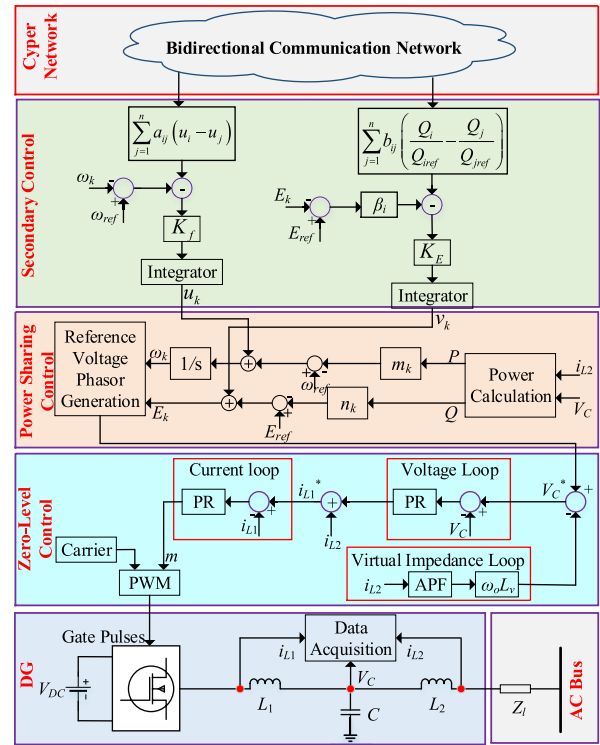
FIGURE 1. Basic schematic of an MG.

time in case of any disturbance. This feature not only enhances voltage and frequency regulation but also ensures accurate power sharing among the DGs;

- A proposed controller with time varying communication delays is implemented in a distributed structure, hence enabling PnP functionality. Moreover, it shows high robustness and efficacy against load variation conditions.

The other parts of this manuscript are organized as follows: The preliminaries, cyber-physical model of an MG, and hierarchical control structure are discussed in Section II. A proposed distributed SC scheme for frequency restoration and active Power (P) sharing in the presence of delays is presented in Section III. In Section IV, a distributed controller for voltage restoration and Reactive Power (Q) sharing is discussed. The performance of the controller scheme is validated under different scenarios, and the results are explained in Section V. Finally, in Section VI, this manuscript is concluded, and future directions are presented.

II. PRELIMINARIES

A DG is usually connected to an MG through a power electronics interface, whose optimal performance is realized through a hierarchical control structure as presented in Fig. 1. Fig. 1 depicts a generalized schematic of the physical layer, zero level control, primary control, SC, and cyber network of the MG system. Therefore, in this section, a detailed discussion is carried out about the physical and cyber system along
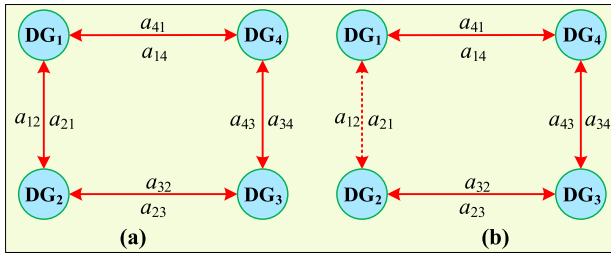
FIGURE 2. Bidirectional connected ring cyber-network (b) Ring cyber-network with CTDs between DG_1 and DG_2.

with the zero and primary control levels, however, a proposed SC level will be explained in the Section III and Section IV.

A. NOTATIONS

Let real numbers set is denoted by $\mathbb{R}$, hence, the notation $\mathbb{R} \geq 0$ represents a set $\{x|x \in \mathbb{R}\}|x \geq 0$, $\mathbb{R} > 0$ denotes a set $\{x|x \in \mathbb{R}\}|x > 0$, and $\mathbb{R} < 0$ defines a set $\{x|x \in \mathbb{R}\}|x < 0$. A null vector is represented by 0_N, while 1_N indicates a vector having all entries are one i.e. $1_N = (1, 1, \ldots\ldots\ldots, 1)^N \in \mathbb{R}^N$.

B. CYBER SYSTEM

A communication network between the DGs serves as a medium for the control signals and measured values to travel in a control system through a cyber-structure. This network can be modelled using a digraph and can be expressed as $G = (\mathbb{N}, \zeta)$, where, $\mathbb{N}$ defines the set of nodes i.e., $\mathbb{N} = \{1, \ldots\ldots.n\}$, and $\zeta = [\mathbb{N}]^2$ as E defines the set of edges i.e., $\zeta = \{e_1, \ldots\ldots., e_m\}$. In the present context, each node is considered as a power unit. The matrix $A = \mathbb{R}^{|N||N|}$ represents an adjacency matrix of G, consisting of elements $a_{kl} = a_{lk} = 1$ if there is an edge exists among the node k and its neighbor l and vice versa, else $a_{kl} = 0$. Also, the degree of the kth node is defined as $D_k = \sum_{k,l\in|N|} a_{kl}$, where $k \neq l$. The Laplacian matrix L of G can be presented as $L = D - A$, where, $D = diag(D_k) \in \mathbb{R}^{|N||N|}$ is the degree matrix. The order of nodes is arranged in such a way that there exists a path called an edge between the nodes k and l. If there is a path exists from node k to node l, the graph is considered to be connected. If Gg is connected, then LL is a positive semidefinite matrix with zero eigenvalue and having an eigenvector is 1_n, i.e., $L1_n = 0_n$ [28].

In the context of this research work, the DGs in the MG are modelled as the nodes in the digraph, whereas the arcs present the communication links between the DGs (with no CTDs), as shown in Fig. 2(a). The Laplacian matrix L that is calculated for the cyber-network based on A and D can be expressed as:

$$A = \begin{bmatrix} 0 & 1 & 0 & 1 \\ 1 & 0 & 1 & 0 \\ 0 & 1 & 0 & 1 \\ 1 & 0 & 1 & 0 \end{bmatrix} \quad (1a)$$

$$D = \begin{bmatrix} 2 & 0 & 0 & 0 \\ 0 & 2 & 0 & 0 \\ 0 & 0 & 2 & 0 \\ 0 & 0 & 0 & 2 \end{bmatrix} \quad (1b)$$

$$L = \begin{bmatrix} 2 & -1 & 0 & -1 \\ -1 & 2 & -1 & 0 \\ 0 & -1 & 2 & -1 \\ -1 & 0 & -1 & 2 \end{bmatrix} \quad (1c)$$

A cyber-network presented in Fig. 2(a) has no CTDs; however, it should be kept in mind that the CTDs are inherent in a cyber-network and are usually due to the network's congested traffic or limited bandwidth. As in the distributed SC, the information and the control tasks are performed through a cyber-network; therefore, in the case of CTDs, each DG receives delayed information from its neighbouring DGs. Let assume that $h_{kl} > 0$ is the communication delay between DG_1 and DG_2 as presented in Fig. 2(b). As a result, the DGs received delayed information from each other, which affected the system performance and may lead to system instability. The details of the impacts of CTDs on the system performance and stability are described in detail in [9]. Hence, based on the above discussion, it is very important to investigate the effects of the CTDs on the SC and how to cope with the problem, which is discussed in detail in the upcoming sections.

C. PHYSICAL SYSTEM

A general meshed MG is considered in this research work and it is assumed to be connected through a digraph as $G = (\mathbb{N}, \zeta)$, i.e., with nodes $\mathbb{N}$ being the DGs (associated phase angle (δ_k) and voltage magnitude (E_k)) and edges ζ being the line impedances. Let consider a network with N-DGs, and assume that the Admittance (Y_{kl}) between the kth-DG and l^{th}-DG can be defined as $Y_{kl} = G_{kl} + jB_{kl} \in \mathbb{C}$; where, $G_{kl} \in \mathbb{R}$ shows the conductance while the susceptance is presented as $B_{kl} \in \mathbb{R}$. If there is no connection between k^{th}-DG and l^{th}-DG, then for convenience, admittance is define as $Y_{kl} = 0$. A set of neighbouring DGs of kth-DG is denoted as $N_k = \{l \,|\, l \in \mathbb{N}, k \neq l, Y_{kl} \neq 0\}$. Furthermore, it is assumed that MG is connected, it means that for all pairs $\{k, l\} \in \mathbb{N} \times \mathbb{N}, k \neq l$, i.e. there exist a sequence of nodes from k to l such that for any two sequential connected consecutive nodes there will be a power line that presented the admittance [29].

Based on these considerations, the injected P and Q according to [30] can be given as:

$$P_k = E_k^2 G_{kk} - \sum_{l=1}^{n} E_k E_l \, |Y_{kl}| \cos(\delta_k - \delta_l - \phi_{kl}) \quad (2a)$$

$$Q_k = -E_k^2 B_{kk} - \sum_{l=1}^{n} E_k E_l \, |Y_{kl}| \sin(\delta_k - \delta_l - \phi_{kl}) \quad (2b)$$

where, $|Y_{kl}| = \sqrt{G_{kl}^2 + B_{kl}^2}$ and the admittance angle of Y_{kl} is presented by ϕ_{kl}. It is assumed that the transmission lines of the MG are lossless and are purely inductive, i.e. $G_{kl} = 0$,

$Y_{kl} = jB_{kl}$, and $\phi_{kl} = \phi_{lk} = -(\pi/2)$. Hence base on these assumption (2) can be written as:

$$P_k = \sum_{l=1}^{n} E_k E_l |B_{kl}| \cos(\delta_k - \delta_l) \tag{3a}$$

$$Q_k = -\sum_{l=1}^{n} E_k E_l |B_{kl}| \cos(\delta_k - \delta_l) + E_k^2 \sum_{l=1}^{n} B_{kl} \tag{3b}$$

Remark 1: The above discussed assumption is reasonable and common in system analysis. A purely inductive lines can be achieved by make the inductive effect more dominant than the resistive effect in a network. A detailed elaboration and justification can be seen in [29] and [31].

D. HIERARCHAL CONTROL STRUCTURE
The control of an MG is generally practiced in a hierarchical manner that composed of primary, secondary, tertiary control levels. A tertiary control level is out of the scope of this research paper therefore it is not discussed in this manuscript. An SC level will be discuss in detail in Section III and IV. A primary control level is discuss in this sub-section that consists of inverter output control or zero control level and power sharing control as shown in Fig. 1. This control level has the fastest response time compared to other control levels and send the control signals at interval of milliseconds to inverter to perform its mandatory control actions.

1) ZERO LEVEL CONTROLLER
The inverter output control consists of an inner control loop that regulates the current and outer control loop that controls the voltage. The control loops are controlled in a decoupled manner; therefore, the dynamic speed of the current loop is 5-20 times faster than the voltage loop. A comprehensive review of the different controllers used in these inner loops can be found in [32]. In this paper, a proportional resonant controller discussed in [33] is used in these loops due to its high tracking capability (sinusoidal references) and dynamic response. This PR controller is designed based on a Naslin polynomial while considering the dynamics of LCL filter. Moreover, a unique equation is derived for every parameter thus avoiding the trial-and-error method and complex trigonometric calculations. Other advantages of this PR controller compared to others include high attenuation, smooth output waveforms, low total harmonic distortion, and fast dynamic response with low computational burden. Furthermore, a virtual impedance loop is applied to make an MG mainly inductive [34].

2) POWER SHARING CONTROLLER
A primary control level is implemented locally in the inverter based MG system and is responsible for regulating the frequency and voltage while ensuring appropriate power sharing. In a conventional power system, a synchronous generator is used to provide this feature. The imbalance between the input mechanical power of the synchronous generator and its

output active power (due to electromagnetic field) causes a change in the speed of the rotor that appears as frequency deviation. Likewise, a variation in the output Q results in variation in the voltage magnitude. Hence, in RES based DGs, a droop controller is used that mimics the characteristics of a synchronous generator due to absence or very low inertia. A most commonly used droop controllers are Active Power-Frequency (P-ω) droop and Reactive Power-Voltage (Q-E) droop controllers that can be expressed as [35]:

$$\omega_k = \omega_{ref} - m_k P_k \tag{4a}$$

$$E_k = E_{ref} - n_k Q_k \tag{4b}$$

where, ω_k and E_k are the operating angular frequency and measured output voltage of the kth-DG respectively ($k = 1, 2, \ldots\ldots, n$), ω_{ref} and E_{ref} are the nominal angular frequency and voltage respectively, m_k and n_k are the P and Q droop coefficients and can be calculated as $m_k = (\omega_{max} - \omega_{min})/P_{max}$ and $n_k = (E_{max} - E_{min})/Q_{max}$ respectively [36].

Although and power sharing and stability of the MG is achieved, but it has some disadvantages such as (a) under critical load, a droop controller accurately manages the Q-sharing but results in week voltage regulation. As voltage is not a global variable in an MG network therefore accurate Q-sharing is a challenge as it results in circulating reactive current, (b) it is not feasible for non-linear loads, as only the fundamental components of current and voltage are taken into account and only measured the averaged value of P and Q while neglecting the harmonics. The non-linear loads results in harmonic current circulation that results in poor power quality, (c) there is a trade-off between accurate power sharing and frequency/voltage deviation. A steeper droop curves result in better power sharing but the same time a large deviation in voltage and frequency from their references is observed. Hence, due to these disadvantages there is an automatic call for the SC level.

III. DISTRIBUTED FREQUENCY REGULATION AND ACTIVE POWER SHARING CONTROLLER
A DAPI based SC for frequency regulation and active power sharing proposed in [37] is given as:

$$\omega_k = \omega_{ref} - m_k P_k + u_k \tag{5a}$$

$$\frac{du_k}{dt} = \left[K_f \left(\omega_{ref} - \omega_k \right) \right] + \left[K_P \left(\sum_{l=1}^{n} a_{kl}(u_l - u_k) \right) \right] \tag{5b}$$

where, u_k is the SC variable; K_f and K_P are the designed constant SC positive gain for f-regulation and P-sharing respectively; $a_{kl} = 1$, if a communication-link among k^{th}-DG and l^{th}-DG exists, otherwise, $a_{kl} = 0$. An adjacency matrix for the frequency regulation and active power sharing is presented as $A = \{a_{kl}\}$.

From (5b), it can be observed that it consists of two parts, i.e., a term $(\omega_k - \omega_{ref})$ is used for frequency regulation and a term $\left(\sum_{l=1}^{n} a_{kl}(u_l - u_k) \right)$ is used for active power sharing.

Moreover, as (5b) is based on distributed architecture therefore the communication among them is performed through a sparse communication network, while the authors consider an ideal communication network, i.e., without any CTDs. Thus, in case of any communication delay, a DG will receive delayed information that can affect the performance of an MG and may lead to system instability. Therefore, based on a DAPI, a new controller is designed that ensure the stability of the system in case of communication delays.

A. DISTRIBUTED FREQUENCY CONTROL SCHEME

A proposed distributed SC for frequency regulation considering CTDs is presented as:

$$\omega_k = \omega_{ref} - m_k P_k + u_k^f \tag{6a}$$

$$\frac{du_k^f}{dt} = K_f \left[\sum_{l=1}^{n} a_{kl} \left(\omega_l(t-\tau) - \omega_k(t) \right) - \left(\omega_k - \omega_{ref} \right) \right] \tag{6b}$$

where, ω_l is the measured angular frequency of the lth-DG ($l = 1, 2,\ldots\ldots, n$); $\tau(t)$ is a time varying delay, $\tau(t) \in [0, h]$ is a bounded time varying delay and $h > 0$ (time delay). From (6b), it can be observed that the main objectives of this research work are to restore the frequency of every DG to its reference value even in the presence of communication delays. Now define the error function as:

$$e_k^f(t) = \omega_k(t) - \omega_{ref} \tag{7}$$

Let assume that all the DGs are connected with each other through digraph and have access to their reference values. Hence, all the DGs must be synchronized with their reference value i.e. ω_{ref} even in the presence of CTDs. Therefore, we can say that $\dot{\omega}_{ref} = 0$. Thus, taking a time derivative of (7) would give us:

$$\dot{e}_k^f(t) = \dot{\omega}_k(t) \tag{8}$$

Combine (6b) and (8) would give us:

$$\frac{du_k^f}{dt} = K_f \left[\sum_{l=1}^{n} a_{kl} \left(e_l^f(t-\tau) - e_k^f(t) \right) - \left(e_k^f(t) \right) \right] \tag{9}$$

To derive the stability conditions for delay independent system, a Lyapunov function for (9) can be given as:

$$V_f(t) = \sum_{k=1}^{n} \left(e_k^f(t) \right)^2 + \sum_{k=1}^{n} \sum_{l=1}^{n} a_{kl} \int_{t-\tau}^{t} \left(e_l^f(s) \right)^2 ds \tag{10}$$

From (10), it is clear that $V_f(t) > 0$; and $V_f(t) = 0$ if and only if $e_k^f(t) = e_l^f(t) = 0$, i.e. $\omega_k(t) = \omega_l(t) = \omega_{ref}$. Now take the derivative of (10) with respect to time along with (9) would yield us to:

$$\dot{V}_f(t) = 2 \sum_{k=1}^{n} e_k^f(t) \dot{e}_k^f(t)$$
$$+ \sum_{k=1}^{n} \sum_{l=1}^{n} a_{kl} \left(\left(e_l^f(t) \right)^2 - \left(e_l^f(t-\tau) \right)^2 \right) \tag{11}$$

Solving (11) would give us:

$$\dot{V}_f(t) = 2 \sum_{k=1}^{n} \sum_{l=1}^{n} a_{kl} e_k^f(t) \left(e_l^f(t-\tau) - e_k^f(t) \right)$$
$$- 2 \sum_{k=1}^{n} \left(e_k^f(t) \right)^2 + \sum_{k=1}^{n} \sum_{l=1}^{n} a_{kl} \left(\left(e_l^f(t) \right)^2 - \left(e_l^f(t-\tau) \right)^2 \right) \tag{12}$$

As the communication graph is balanced, thus:

$$\sum_{k=1}^{n} \sum_{l=1}^{n} a_{kl} \left(e_k^f(t) \right)^2 = \sum_{k=1}^{n} \sum_{l=1}^{n} a_{kl} \left(e_l^f(t) \right)^2 \tag{13}$$

Apply (13) in (12) would give us:

$$\dot{V}_f(t) = - \sum_{k=1}^{n} \sum_{l=1}^{n} a_{kl} \left(e_k^f(t) - e_l^f(t-\tau) \right)^2$$
$$- 2 \sum_{k=1}^{n} \left(e_k^f(t) \right)^2 \tag{14}$$

From (14), it can be observed that $\dot{V}_f(t)$ can either be zero or less than zero. If in case $\dot{V}_f(t) = 0$ we get $e_k^P(t) = 0$ and $e_k^P(t) = e_l^P(t-\tau)$, however when $\dot{V}_f(t) < 0$ then it means that the frequencies of the DGs converges to ω_{ref} asymptotically.

Remark 2: At a steady-state the secondary control input u_k is activated and can be directly calculated from (6b) as $u_k^f = \int_{t_0}^{t} K_f \left[\sum_{l=1}^{n} a_{kl} \left(\omega_l(t-\tau) - \omega_k(t) \right) - \left(\omega_k(t) - \omega_{ref} \right) \right] dt$. At a new steady-state i.e. $\omega_k = \omega_{ref}$, then in the context of (6a) we have $\int_{t_0}^{t} K_f [\sum_{l=1}^{n} a_{kl}(\omega_l(t-\tau) - \omega_k(t)) - (\omega_k(t) - \omega_{ref})] dt = \omega_k - \omega_n + m_k P_k$. Hence, we can say that a new bounded compensation term i.e. u_k^f is added for restoration of system's frequency to their reference value.

1) UPDATE THE VALUE OF K_f

A distributed SC presented in (6b) has fixed gain parameter i.e. K_f. Due to this fixed parameter a controller will not be able to accurately regulate the frequency to its nominal values in case of any disturbance or uncertainty (it can also be seen in the simulation results in [37]). Hence, to cope with this problem, a Massachusetts Institute of Technology (MIT) rule based adaptive control technique is develop that update the value of K_f in every sampling time such that the system perform efficiently in case of any uncertainty such as PnP, load variation etc. To make K_f adaptive a following assumption is made.

Assumption 1: Consider a controller in (6a) can be described in (15a) and (15b) that shows the current and updated values as:

$$\omega_S = \omega_{ref} + k_S^f u_S^f - m_k P_k \tag{15a}$$

$$\omega = \omega_{ref} + k^f u^f - m_k P_k \tag{15b}$$

where, k_S^f and k^f denotes the current and updated values of gain respectively. Applying the update control law $u^f = \xi u_S^f$ in (15b) would give us:

$$\omega = \omega_{ref} + k^f \xi u_S^f - m_k P_k \tag{16}$$

where, u_S^f and u^f denotes the previous and updated control input while ξ is the adjustment parameter. Moreover, it is the considered that the updated error e_S^f can be define as $e_S^f = \omega - \omega_S$. Now put (15a) and (16) in the error function and take derivative; we get:

$$\dot{e}_S^f = \dot{\omega}_{ref} + k_S^f \dot{u}_S^f - m_k \dot{P}_k - \dot{\omega}_{ref} - k^f \xi \dot{u}_S^f + m_k \dot{P}_k \tag{17}$$

Solution of (17) would yield us to:

$$\dot{e}_S^f = k_S^f \dot{u}_S^f - k^f \xi \dot{u}_S^f \tag{18}$$

As discussed above at a steady-state $e_S^f = 0$, thus as a result $\dot{e}_S^f = 0$. Hence, $\xi = k_S^f \big/ k^f$.

Keeping the above discussed assumption and consider a system in (6b), an MIT rule according to [38] can be expressed as:

$$J(\xi) = \frac{1}{2}\left(e_S^f\right)^2 \tag{19}$$

where, in (19) the adjustment parameter ξ minimizes the loss function, therefore, the parameters can be can in the negative direction of gradient of J; thus, it can be given as:

$$\frac{d\xi}{dt} = -\lambda_f \frac{\partial J}{\partial \xi} \tag{20}$$

where, λ_f is the learning parameter and $\frac{\partial J}{\partial \xi} = \frac{\partial J}{\partial \omega} \cdot \frac{\partial \omega}{\partial u^f} \cdot \frac{\partial u^f}{\partial \xi} = \xi\left(e_S^f\right)^2$. Put this in (20) would give us:

$$\frac{d\xi}{dt} = -\lambda_f \xi \left(e_S^f\right)^2 \tag{21}$$

Hence, based on this rule the SC in (6b) can be updated as:

$$\frac{du_k^f}{dt} = \left[-\lambda_f \xi \left(e_S^f\right)^2\right]$$
$$\left[\sum_{l=1}^{n} a_{kl}\left(\omega_l(t-\tau) - \omega_k(t)\right) - \left(\omega_k - \omega_{ref}\right)\right] \tag{22}$$

B. ACTIVE POWER SHARING CONTROLLER

An active power sharing controller considering CTDs can be given as:

$$\frac{du_k^P}{dt} = K_P \left[\sum_{l=1}^{n} a_{kl}\left(u_l^P(t-\tau) - u_k^P(t)\right)\right] \tag{23}$$

For simplicity, consider the dynamics in (23) in vector form along with the CTDs and can be expressed as:

$$\frac{du_k^P}{dt} = X_P u(t) + X_{P-1} u(t-\tau(t)) \tag{24}$$

where, X_P and X_{P-1} are constant positive $n \times n$ matrices. In this research work, the stability conditions are derived

by using Razumikhin's method and applying a Lyapunov function. Let a Lyapunov function given below as:

$$V_P(u_t) = u^T(t) G_P u(t) \tag{25}$$

where, G_P is positive $n \times n$ matrices i.e. $G_P > 0$ and are positive definite and symmetric. Consider a derivative of V_P along (24). We will apply the Lyapunov Razumikhin's technique $\bar{\sigma}_P(s) = \bar{\sigma}_P.s$, where a constant $\bar{\sigma}_P > 1$. According to Razumikhin's theorem [39], [40], when the condition:

$$\bar{\sigma}_P u^T(t) G_P u(t) - u^T(t-\tau(t)) G_P u(t-\tau(t)) \geq 0 \tag{26}$$

holds for some constant $\bar{\sigma}_P = 1 + \vartheta_P$, where, $\vartheta_P > 0$, it can be concluded that for any $\aleph_P > 0$, there exists $\beta_P > 0$ such that:

$$\begin{aligned}
\dot{V}_P(u(t)) &= 2u^T(t) G_P \left[X_P u(t) + X_{P-1} u(t-\tau(t))\right] \\
&\leq 2u^T(t) G_P \left[X_P u(t) + X_{P-1} u(t-\tau(t))\right] \\
&\quad + \aleph_P \left[\bar{\sigma}_P u^T(t) G_P u(t) - u^T(t-\tau(t)) \right. \\
&\quad \left. G_P u(t-\tau(t))\right] \\
&\leq -\beta_P |u(t)|^2
\end{aligned} \tag{27}$$

if

$$\begin{bmatrix} X_P^T G_P + G_P X_P + \aleph_P G_P & G_P X_{P-1} \\ X_{P-1}^T G_P & -\aleph_P G_P \end{bmatrix} < 0 \tag{28}$$

From (27) and (28), it can be observed that the matrix inequality does not depend on the delay derivative term as there is no constraint on the delay derivative. Hence, the feasibility of (27) is sufficient for the delay independent stability of an MG having CTDs and provide a sufficient condition for the asymptotical stability of the system.

1) SENSITIVITY ANALYSIS
Take the Laplace transform of (23) would give us:

$$s u_k^P - u_k^P(0) = K_P \sum_{l=1}^{n} a_{kl} \left(u^{-\tau ls} u_l^P(s) - u_k^P(s)\right) \tag{29}$$

Let $U(s) = u_1^P(s), u_2^P(s), \ldots\ldots\ldots, u_n^P(s)$. Then we get,

$$U(0) = (sI_N + K_{P2}A_0 - K_{P1}A_\tau(s)) U(s) \tag{30}$$

where, A_τ is a matrix having entries $a_{kl}(s) = a_{kl}u^{-\tau ls}$ and matrix $A_0 = diag\{d_k\}$. To make the analysis simple it is assume that $\tau_1 = \tau_2 = \ldots\ldots\ldots = \tau_n = \tau$. According to [41] and analogous to the case of finite dimensions, the characteristics equation can be written as:

$$\Delta(s) = sI_N + K_{f2}A_0 - K_f u^{-\tau s}A \tag{31}$$

As the spectrum of (31) is associated with communication delays, an approximation technique discussed in [42] is adopted to analyze (31) i.e., the eigenvalues of discretization matrix W can be given as:

$$W = \frac{\widehat{\mathbb{C}} \otimes I_N}{K_{f2}A_1 \; 0 \; \ldots\ldots \; 0 \; -K_{f2}A_0} \tag{32}$$

where, $\otimes$ is the Kronecker product, I_N is the identity matrix of order n, the denominator presents the boundary conditions (i.e. $-\tau$ to 0), the matrix $\widehat{\mathbb{C}}$ consists of first n rows of the matrix $\mathbb{C}$ and is described as:

$$\mathbb{C} = -\frac{2D_n}{\tau} \tag{33}$$

where, D_n is defined as the Chebyshev's differentiation matrix of the order $(n+1) \times (n+1)$. Initially, $(n+1)$ Chebyshev's nodes are define i.e., the interpolation points on the normalized interval $[-1, 1]$ and are given as:

$$z_\gamma = \cos(\gamma\pi/n) \tag{34}$$

where, $\gamma = 0, 1.2, \ldots\ldots, n$, and entries of D_n are shown as:

$$D_{(k,l)} = \begin{cases} \dfrac{\mathbf{c}_k (-1)^{k+l}}{\mathbf{c}_j (z_k - z_l)}, & k \neq l \\ -\dfrac{z_k}{2(1 - z_k^2)}, & k = l \neq 0, n \\ \dfrac{2n^2 + 1}{6}, & k = l = 0 \\ -\dfrac{2n^2 + 1}{6}, & k = l = n \end{cases} \tag{35}$$

where, $\mathbf{c}_0 = \mathbf{c}_n = 2$ and $\mathbf{c}_1 = \mathbf{c}_2 = \ldots\ldots = \mathbf{c}_{n-1} = 1$.

From the above notion, it can be concluded that the eigenvalues will appear on the left side of the plane that explains that a system will remain stable even for the large CTDs. Moreover, it is also noted that as the time delay swells, the effects are more prominent as can be seen in Appendix A.

2) UPDATE THE VALUE OF K_P

To update the value of K_P in every sampling time such a controller perform efficiently and ensure an accurate active power sharing in case of any system disturbance or uncertainty in this subsection a Back Propagation (BP) based Adaptive PI (API) controller will be presented. A traditional PI controller can be expressed as:

$$K_P = k_{P-p}(t) e^P(t) + k_{P-i}(t) \int_0^t e^P(t) dt \tag{36}$$

To update the fixed SC gain parameter i.e. K_P in P-sharing controller i.e. in (23), a BP based API controller is designed in which an error is minimized by using a gradient descent function and is given as:

$$J = \frac{1}{2}(e_P)^2(t) \tag{37}$$

where, $e_P = P_k - P_{ref}$. The updated esteemed gain values of PI controller $k_{P-p}(t+1)$ and $k_{P-i}(t+1)$ can be given as:

$$k_{P-p}(t+1) = k_{P-p}(t) + k_{P-pnew}(t) \tag{38a}$$

$$k_{P-i}(t+1) = k_{P-i}(t) + k_{P-inew}(t) \tag{38b}$$

where, $k_{P-pnew}(t)$ and $k_{P-inew}(t)$ are the new proportional and integral gains of PI controller and can be calculated as:

$$k_{P-pnew}(t) = -\lambda_P \frac{dJ}{dt} = -\lambda_P \left(\frac{\partial J}{\partial P}.\frac{\partial P}{\partial u^P}.\frac{\partial u^P}{\partial k_{P-p}}\right)$$
$$= -\lambda_P e_P^2(t) k_{P-p}(t) \tag{39a}$$

$$k_{P-inew}(t) = -\lambda_P \frac{dJ}{dt} = -\lambda_P \left(\frac{\partial J}{\partial P}.\frac{\partial P}{\partial u^P}.\frac{\partial u^P}{\partial k_{P-i}}\right)$$
$$= -\lambda_P e_P^2(t) k_{P-i}(t) \tag{39b}$$

By putting the values of $k_{P-pnew}(t)$ and $k_{P-inew}(t)$ in (38a) and (38b) respectively, we get:

$$k_{P-p}(t+1) = k_{P-p}(t)\left(1 - \lambda_P e_P^2(t)\right) \tag{40a}$$

$$k_{P-i}(t+1) = k_{P-i}(t)\left(1 - \lambda_P e_P^2(t)\right) \tag{40b}$$

Based on these equations, (36) can be updated as:

$$K_P = \left[\left\{k_{P-p}\left(1 - \lambda_P e_P^2(t)\right)\right\} e_P(t)\right]$$
$$+ \left[\left\{k_{P-i}\left(1 - \lambda_P e_P^2(t)\right)\right\} \int_0^t e_P^2(t) dt\right] \tag{41}$$

Hence, the SC for P-sharing presented in (23) can be given as:

$$\frac{du_k^P}{dt} = \begin{bmatrix} \left[\left\{k_{P-p}\left(1 - \lambda_P e_P^2(t)\right)\right\} e_P(t)\right] + \\ \left[\left\{k_{P-i}\left(1 - \lambda_P e_P^2(t)\right)\right\} \int_0^t e_P^2(t) dt\right] \end{bmatrix}$$
$$\left[\sum_{l=1}^n a_{kl}\left(u_l^P(t-\tau) - u_k^P(t)\right)\right] \tag{42}$$

IV. DISTRIBUTED VOLTAGE REGULATION AND REACTIVE POWER SHARING CONTROLLER

In this subsection SC will be discussed that ensures accurate Q-sharing and regulate the voltage in the presence of CTDs.

A. DISTRIBUTED VOLTAGE CONTROL SCHEME

A distributed SC for E-regulation considering CTDs is presented as:

$$E_k = E_{ref} - n_k Q_k + v_k \tag{43a}$$

$$\frac{dv_k}{dt} = K_E \left[\sum_{l=1}^n b_{kl}(E_l(t-\tau) - E_k(t)) - \Omega_k(E_k - E_{ref})\right] \tag{43b}$$

where, v_k is the SC variable; K_E and Ω_k are the designed SC positive gain. Moreover, if a communication-link between k^{th}-DG and l^{th}-DG is present then $b_{kl} = 1$, otherwise $b_{kl} = 0$. An adjacency matrix is presented as $B = \{b_{kl}\}$ and to avoid extra communication channel for simplicity it is considered that $B = A \Rightarrow \{b_{kl}\} = \{a_{kl}\}$.

A detail proof of voltage regulation is discussed in Appendix B. Moreover, from (43) it can be concluded that:

Remark 3: As the graph between the DGs is balanced and connected then consider the primary voltage controller presented in (43a) having a control input v_k for the secondary controller then the voltage (E_k) of every DG synchronize to its reference (E_{ref}) even in the presence of CTDs.

Furthermore, to update the SC fixed gain parameter i.e. K_E an adaptive controller based on MIT rule is used similar to
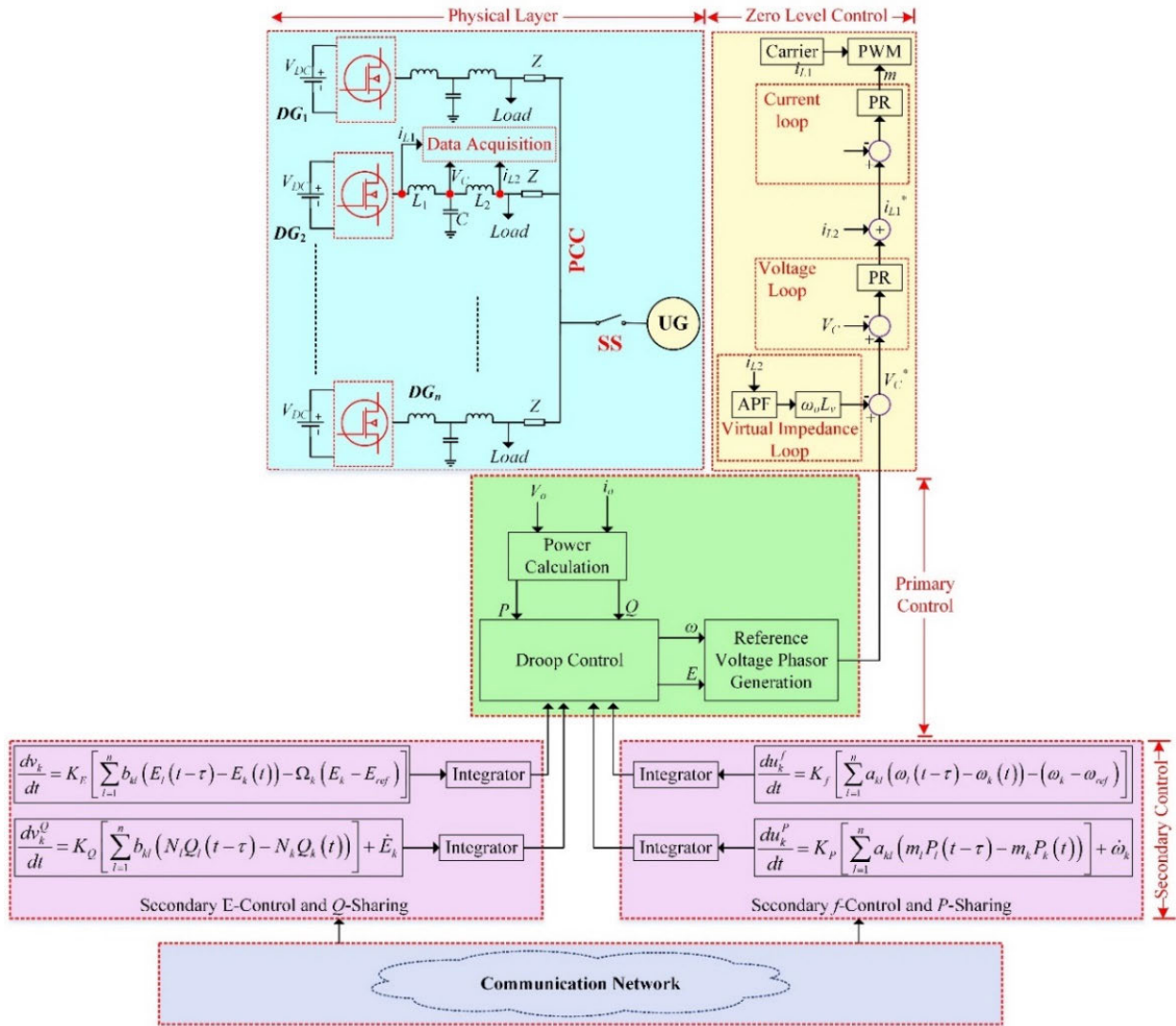
FIGURE 3. Schematic of distributed control structure.

that applied to update K_f that can be omitted here. We get our finalized expression as:

$$\frac{dv_k}{dt} = \left[-\lambda_E \xi \left(e_S^f \right)^2 \right] \left[\sum_{l=1}^{n} b_{kl} \left(E_l \left(t - \tau \right) - E_k \left(t \right) \right) - \Omega_k \left(E_k - E_{ref} \right) \right]$$

(44)

B. REACTIVE POWER SHARING CONTROLLER

A reactive power sharing controller considering CTDs can be given as:

$$\frac{dv_k^Q}{dt} = K_Q \left[\sum_{l=1}^{n} b_{kl} \left[\left(Q_l \left(t - \tau \right) \right) - \left(Q_k \left(t \right) \right) \right] \right]$$

(45)

where, K_Q is the designed SC gain. Moreover, $Q_k = Q_{kmea} / Q_{kref}$ and $Q_l = Q_{lmea} / Q_{lref}$ in which Q_{kmea} and

Q_{lmea} are the measured injected reactive power of kth-DG and l^{th}-DG respectively, while Q_{kref} and Q_{lref} are the kth-DG and l^{th}-DG reactive power ratings.

A detailed proof of Q-sharing can be seen in Appendix C. Moreover, to update the Q-sharing SC fixed gain parameter i.e. K_Q, an adaptive controller based on BP technique is used and its proof is same as discussed for updating the K_P and can be expressed as:

$$\frac{dv_k^Q}{dt} = \left[\begin{array}{c} \left[\left\{ k_{P-p} \left(1 - \lambda_Q e_P^2 \left(t \right) \right) \right\} e_P \left(t \right) \right] + \\ \left[\left\{ k_{P-i} \left(1 - \lambda_Q e_P^2 \left(t \right) \right) \right\} \int_0^t e_P^2 \left(t \right) dt \right] \end{array} \right] \left[\sum_{l=1}^{n} b_{kl} \left[\left(Q_l \left(t - \tau \right) \right) - \left(Q_k \left(t \right) \right) \right] \right]$$

(46)

Remark 4: The secondary control gains parameters i.e. $K_f, K_P, K_E,$ and K_Q are made adaptive that are used for the tuning of the convergence rates of secondary frequency,
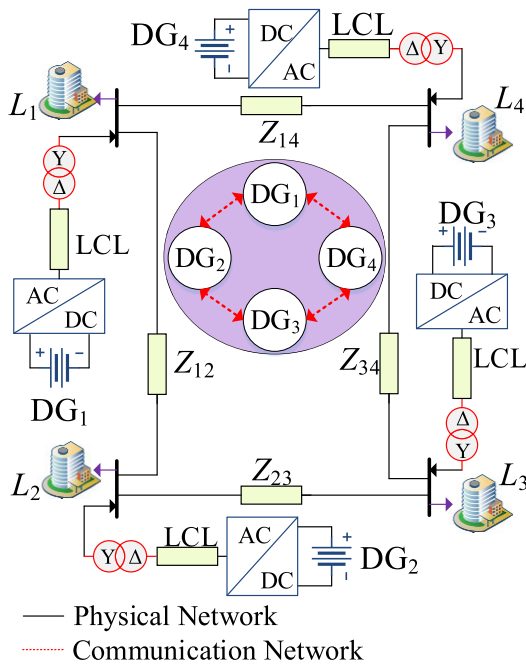
FIGURE 4. Schematic of an MG under consideration.

TABLE 2. Parameters Of MG test system.

Parameter	Symbol	Value
Primary Controller Parameters		
Droop coefficients	m_i (P-ω)	10^{-5} rad / (W s)
	n_i (Q-E)	10^{-3} V/Var
Secondary Controller Parameters		
SC f-P gains	K_f	0.1
	K_P	0.13
SC E-Q gains	K_E	0.01
	K_Q	0.015
Learning rate	λ_f	2.4
	λ_P	3.6
	λ_E	2.7
	λ_Q	3.1
Electrical Parameters		
Nominal Voltage	E	310 V
Frequency	Nominal f	50 Hz
	Switching f_{sw}	10×10^{-3}Hz
	Sampling f_a	$1/1\times10^{-6}$ Hz
Line Impedance	Z_{12}	0.9 Ω + 4 mH
	Z_{23}	1.2 Ω + 5 mH
	Z_{34}	0.8 Ω + 3 mH
	Z_{14}	1.6 Ω + 6 mH
Load (P+Q)	L_1= L_2= L_3= L_4	1 kW + 1 kVar
LCL Filter Parameters		
Inverter-side inductor	L_i	1.74×10^{-4} H
Grid-side inductor	L_g	1.2×10^{-3} H
LCL capacitance	C_f	3.31×10^{-5} F

voltage, active and reactive power sharing respectively. It should be noted that both the controllers, i.e., MIT rule based adaptive controller and BP based API can be used to update any of the above secondary control gain parameters i.e. K_f, K_P, K_E, and K_Q.

Remark 5: The frequency and voltage deviation caused by the droop based primary controller and ensure accurate power
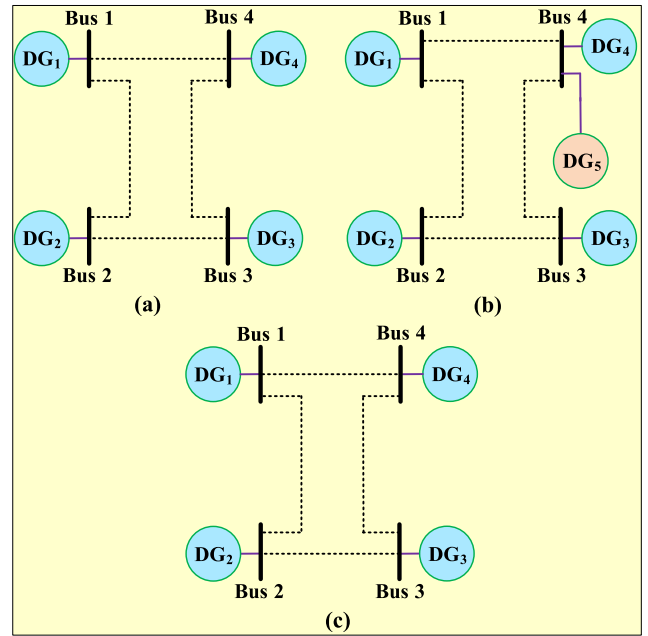

FIGURE 5. MG physical network topology during (a) normal operation (b) DG$_5$ plug-in (c) DG$_5$ plug-out.

sharing, the SC laws u_k^f, u_k^P, v_k^E, and v_k^Q are designed in this work. Similar to [37] these SC variables are added directly to the primary controller.

A detailed schematic of the proposed distributed control structure is shown in Fig. 3.

V. PERFORMANCE VALIDATION

The performance of the proposed distributed SC is validated through simulations that are performed in MATLAB/ SimPower software. A MG under consideration consists of four DGs (DG$_1$-DG$_4$), four local loads (L_1-L_4), and four transmission lines whose impedances are labelled as (Z) as presented in Fig. 4. The values of the parameter used in this study are tabulated in Table 2. The performance and effectiveness of the controller is examined in different scenarios that are elaborated below.

A. PLUG-AND-PLAY CAPABILITY

As the renewable energy generating units are intermittent in nature, as a result they can be plugged-in and plugged-out at any instant. Therefore, an MG must have the capability to perform PnP functionality. In other words, a distributed MG allows an existing DG to plug-out and permits a new DG to plug-in without redesigning an MG. Therefore, the controller must effectively perform the PnP functionality and achieve consensus among the DGs while ensuring system stability. To validate the performance of the proposed controller, in this scenario, it is considered that a DG$_5$ is plugged-in to bus 4 at t = 2 sec and plugged-out at t = 4 sec. During the PnP operation the physical as well as the cyber network of the MG system changes as presented in Fig. 5 and Fig. 6 respectively. To demonstrate the effectiveness of the proposed controller
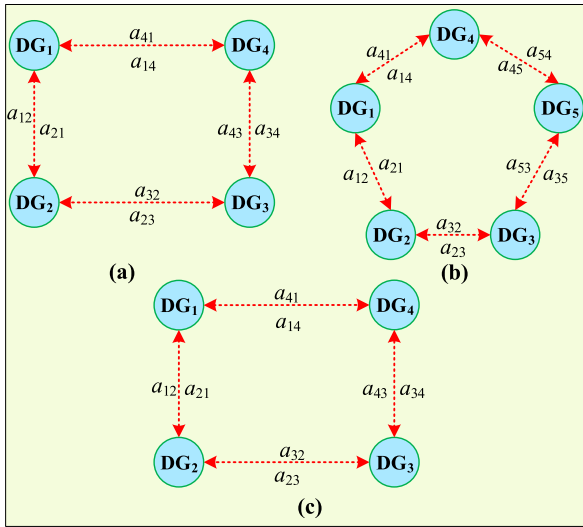
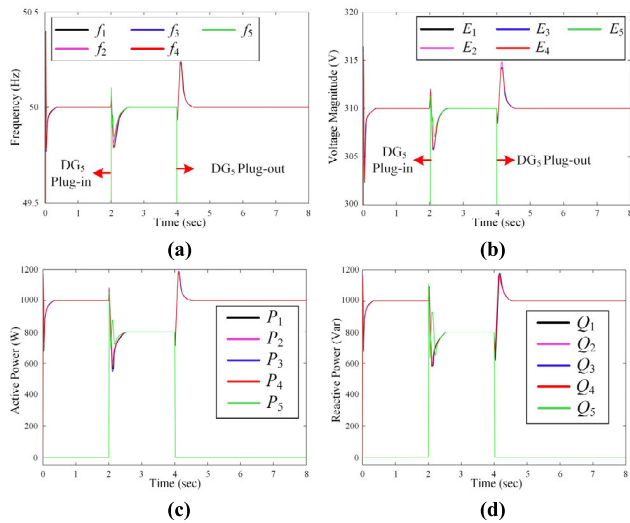**FIGURE 6.** MG communication network topology during (a) normal operation (b) DG$_5$ plug-in (c) DG$_5$ plug-out.

FIGURE 7. Performance of the controller under PnP operation with small CTDs (τ = 0.05 sec) (a) f, (b) E, (c) P, and (d) Q.

FIGURE 8. Performance of the controller under PnP operation with large CTDs (τ = 0.5 sec) (a) f, (b) E, (c) P, and (d) Q.

TABLE 3. Load variation with respect to time.

Time Period		$0 \leq t \leq 2$	$2 \leq t \leq 4$	$4 \leq t \leq 8$
	L_1	1 kW + 1 kVar	.5 kW + .5 kVar	1 kW + 1 kVar
Loads	L_2	1 kW + 1 kVar	.5 kW + .5 kVar	1 kW + 1 kVar
	L_3	1 kW + 1 kVar	2 kW + 2 kVar	1 kW + 1 kVar
	L_4	1 kW + 1 kVar	2 kW + 2 kVar	1 kW + 1 kVar

controller's performance under PnP operations having large CTDs, the τ is selected as 0.5 sec. The simulation results of this case with $\tau = 0.5$ sec are presented in Fig. 8. From Fig. 8, it can be seen that even with the large delays, the proposed controller regulates the voltages and frequencies of the DGs and maintains power consensus. Although high deviations from the references are observed in the output waveforms but the controller responds effectively and achieves stability.

B. ROBUSTNESS TO LOAD VARIATION

In an MG the load varies at any instant based on consumer demands therefore it is very important for the controller to maintain the MG stability in case of sudden load variation. Therefore, in this scenario, the performance of the controller is validated for varying load conditions under slow and fast varying communication delays. Initially, all the loads, i.e., $L_1 = L_2 = L_3 = L_4 = 1$ kW + 1 kVar, are set for $0 \leq t \leq 2$ sec. Then, during the time $2 \leq t \leq 4$ sec, all the loads vary, i.e., $L_1 = L_2 = 0.5$ kW + 0.5 kVar (becomes half) and $L_3 = L_4 = 2$ kW + 2 kVar (becomes double). At t = 4 sec, all the load varies again and comes to its initial state, i.e., $L_1 = L_2 = L_3 = L_4 = 1$ kW + 1 kVar. For simplicity the load variation with respect to time is presented in Table 3.

In the presence of small CTDs i.e. $\tau = 0.05$ sec, when the load varies at t = 2 sec, some deviations in frequency and voltage waveforms from their references in observed but the proposed controller restores these deviations to their nominal

during PnP operation, the simulation tests are conducted considering small and large CTDs.

Initially, small communication delays, i.e., $\tau = 0.05$ sec are considered to show the effectiveness of the proposed controller, as presented in Fig. 7. It can be observed that at t =2 sec, when a DG$_5$ is plugged-in into the system, some deviation in frequencies and voltages of the DGs is observed, but the controller stabilizes these deviations very effectively, and at about 0.4 sec, they come to their reference values. At the same time, when DG$_5$ is plugged-in, the controller achieves a new power consensus and shares the load among the DGs. Similarly, at t = 4 sec, when a DG$_5$ is plugged-out, same frequencies and voltages deviations are observed but the controller responds effectively and reach to their reference levels very rapidly.

Fig. 7 shows that the controller performs very effectively for small communication time delays; however, to show the
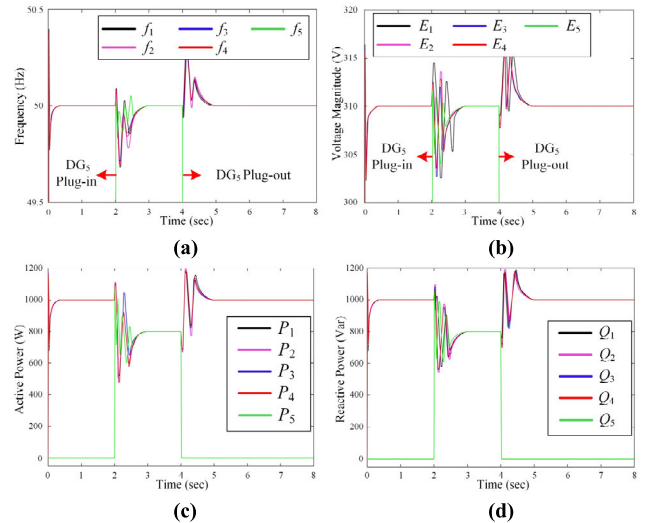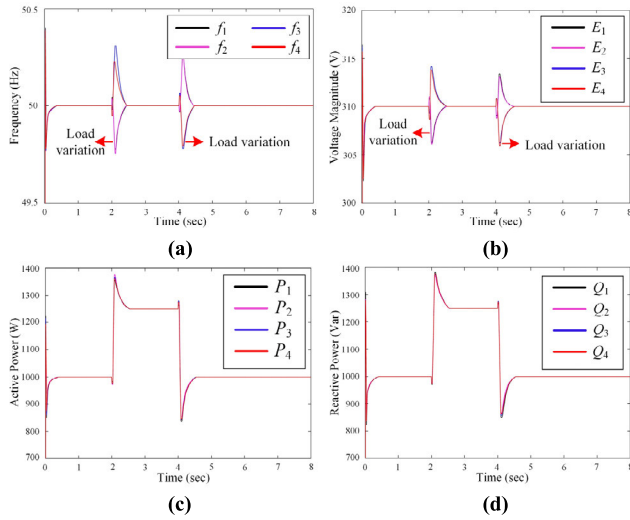
FIGURE 9. Performance of the controller under load variation with small CTDs ($\tau = 0.05$ sec) (a) f, (b) E, (c) P, and (d) Q.
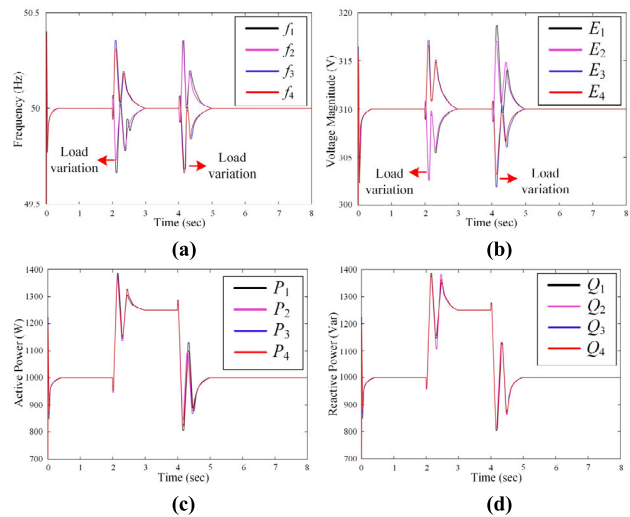

FIGURE 10. Performance of the controller under load variation with large CTDs ($\tau = 0.5$ sec) (a) f, (b) E, (c) P, and (d) Q.

FIGURE 11. Performance of controller under different CTDs (a) f, (b) E, (c) P, and (d) Q.
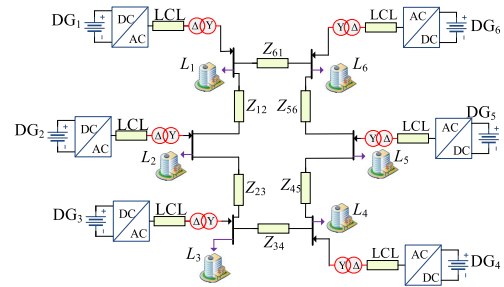
FIGURE 12. Schematic of a large MG under consideration for this case study.

reference values very rapidly as can be seen in Fig. 9(a) and 9(b) respectively. It can be seen that as the load varies, a small deviation is observed in frequency, i.e., around 0.2 Hz, and voltage, i.e., around 3.5 V in the output waveforms. These deviations are restored by the controller very effectively and come to their reference level within 0.55 sec. Moreover, when the load varies a new power consensus is generated and is attained by the controller efficiently, and shares the load among all the DGs as shown in Fig. 9(c) and 9(d).

Similarly, in the case of large CTDs, i.e., $\tau = 0.5$ sec, an MG is subjected to the same pattern of load variation. The output waveforms during large time varying delays are presented in Fig. 10. In Fig. 10, the same frequencies and voltages deviations are observed at an instant when the load varies. But the controller restores these deviations, and approximately within 1.1 sec, they come to a steady-state with a maximum deviation of 0.4 Hz in frequency and 8.5 V in voltage.
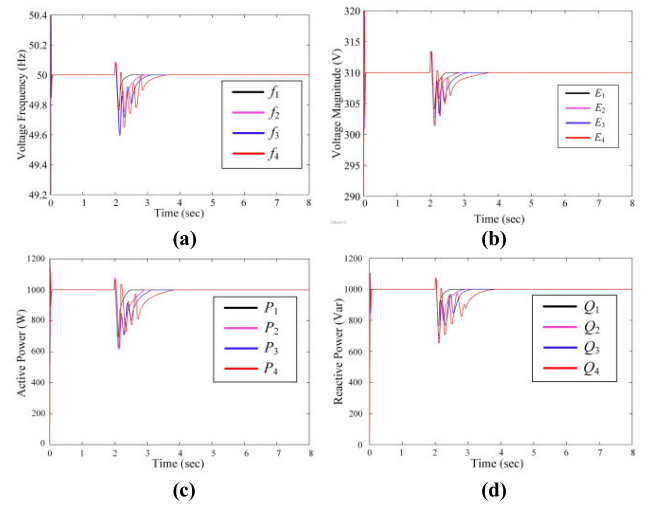
C. CONTROLLER PERFORMANCE UNDER DIFFERENT CTDS

To validate the performance of the proposed controller, in this scenario, it is considered that all the DGs are subjected to different CTDs. The CTDs are set as $\tau_1 = 0.05$ sec, $\tau_2 = 0.3$ sec, $\tau_3 = 0.5$ sec, and $\tau_4 = 0.7$ sec and are introduced at $t = 2$ sec. When these CTDs are subjected, a proposed controller effectively restores the DGs frequencies and voltages to their reference values while attaining accurate power sharing as can be seen in Fig. 11. From Fig. 11, it can be observed that when the CTD is small i.e. $\tau_1 = 0.05$ sec, the controller shows high performance and restores the deviations in the waveforms to their references within 0.55 sec. However, if large CTDs i.e. $\tau_4 = 0.7$ sec, is introduced than compared to small CTDs, performance degradation is observed. But the controller effectively restores the voltage and frequency of DG_4 and within 1.7 sec, the waveforms comes to its steady-state. From Fig. 11, it can be observed when the system is subjected to different CTDs, although some deviations are observed in the output waveforms but the controller stabilizes these deviations rapidly.

D. CONTROLLER PERFORMANCE IN LARGE SYSTEMS

To validate the performance of proposed controllers, in this scenario, a large MG is considered that consists of 06 DGs as
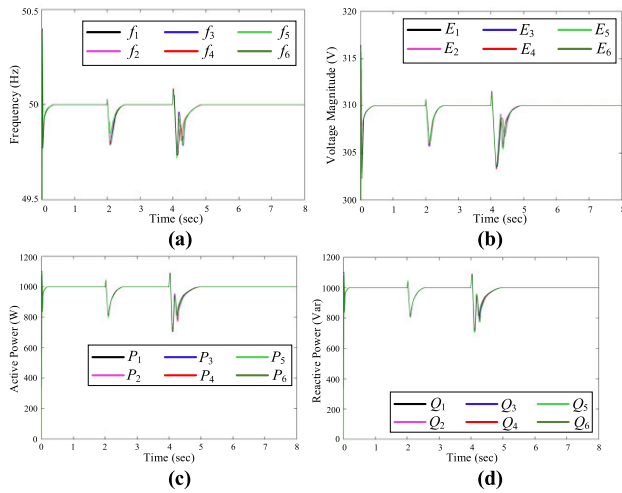
FIGURE 13. Performance of controller under different CTDs in a large MG (a) f, (b) E, (c) P, and (d) Q.

FIGURE 14. Performance of a distributed finite time controller without buffer compensator [14] (a) f, (b) E, (c) P, and (d) Q; ($\tau = 0.2$ sec).

shown in Fig. 11. It is assumed that at t = 2 sec, all the DGs are subjected to CTDs, i.e., $\tau_1 = \tau_2 = \tau_3 = \tau_4 = \tau_5 = \tau_6 = 0.06$ sec. Upon the introduction of CTDs, a deviation in the output waveforms is observed but the proposed controllers effectively restore these deviations, and at about 0.65 sec, they comes to its steady state. Similarly, at t = 4 sec, another set of CTDs, i.e., $\tau_1 = \tau_2 = \tau_3 = \tau_4 = \tau_5 = \tau_6 = 0.25$ is subjected to the system. Although these CTDs cause a deviation in frequencies, voltages, and power waveforms but the controllers restore these deviations effectively, as presented in Fig. 13.

As the proposed controller is based on distributed architecture, it requires only the information of its adjacent neighbouring DGs to perform its control actions. Due to this advantageous feature, the proposed controller shows high flexibility and scalability. Therefore, it can perform effectively in a large systems or in an MG system where numerous multiple DGs are connected. Moreover, the proposed controller are delay-independent as discussed above, therefore, it has the ability to restore the system to its nominal values if the delays are large enough.

E. COMPARISON STUDY
To validate the effectiveness of the proposed controller, its performance is compared with the distributed finite time controller proposed in [14]. It should be noted that in this comparison study, the proposed controller is compared with the finite time controller (i.e., [14]), when the finite time controller did not use any buffer or compensator to mitigate the effect of CTDs. As the proposed controller avoids the use of any compensator to mitigate the effects of CTDs, however, most of the control strategies, such as [12], [14], [18], [19], [23], [24], [25], and [26], use the compensator; therefore, this comparison study shows the advantage of the proposed controller over these controllers.

In this case, CTDs are set as $\tau_1 = \tau_2 = \tau_3 = \tau_4 = \tau = 0.2$ sec and are introduced at t = 2 sec. Due to CTDs, the controller presented in [14] is unable to regulate the frequencies
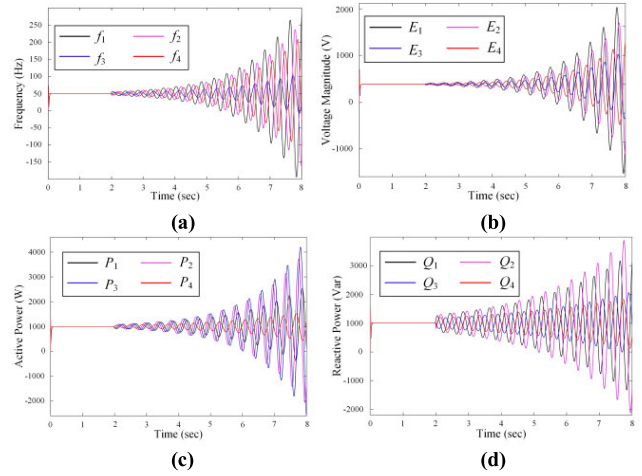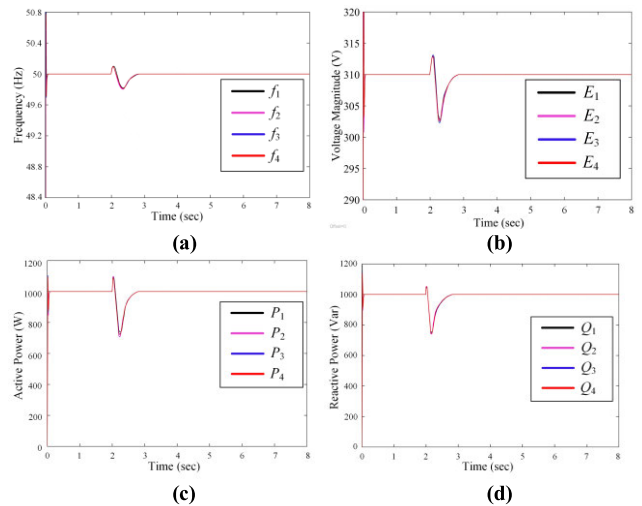

FIGURE 15. Performance of proposed controller with communication delays $\tau = 0.2$ sec (a) f, (b) E, (c) P, and (d) Q.

and voltages of DGs and does not ensure appropriate power sharing as presented in Fig. 14. From Fig. 14, it can be observed that when communication delays are introduced, the controller is unable to handle the delay disturbance and moves towards instability. Therefore, to ensure the stability of the system, a finite time controller uses buffers for delay compensation. Although the usage of a buffer ensure system stability but it is not desirable as it requires storage memory, high computation processor, increases controller complexity, and consumes more electrical power [24].

Therefore, to cope with this challenge, in this research work, a delay independent distributed secondary is proposed that avoids the use of a buffer and ensures system stability. When a proposed controller is subjected to the same communication delays, i.e., $\tau = 0.2$ sec, then the controller effectively restores the DGs frequencies and voltages and ensures appropriate power sharing as presented in Fig. 15. Although some deviations are observed in the output waveforms but the controller stabilizes these deviations to
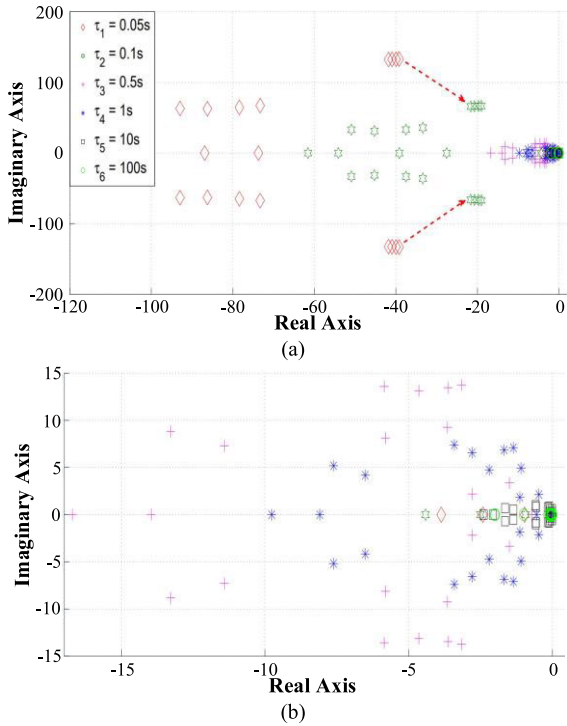
FIGURE 16. Impact of communication TVDs on root loci, *n* = 5 (a) zoom-out view and (b) zoom-in view.

their reference value without using any delay compensation scheme.

VI. CONCLUSION

A delay independent DAPI control scheme incorporated in an MG system for frequency and voltage regulation and power sharing in the presence of CTDs is proposed in this manuscript. The proposed control scheme minimizes the error, maintains system frequency and voltage at reference values, and ensures appropriate power sharing, although small and large communication delays were subjected. Moreover, the stability of the system is ensured without using any delay compensation scheme. To validate the efficacy of the proposed method, simulations are performed in the MATLAB/Sim Power Systems toolbox. The results show that the voltages and frequencies of the DGs are restored to their references very effectively while ensuring appropriate power sharing under PnP operation and load variation conditions. In the future, it is aimed to investigate the distributed secondary control scheme considering stochastic communication delays [43] and network attacks [44].

APPENDIX A
IMPACT OF COMMUNICATION DELAYS
See Figure 16.

APPENDIX B
DISTRIBUTED VOLTAGE CONTROL SCHEME
Define the error function as:

$$e_k^E(t) = E_k(t) - E_{ref} \qquad (47)$$

Let assume that all the DGs are connected with each other through digraph and have access to their reference values. Hence, all the DGs must be synchronized with their reference value i.e. E_{ref} even in the presence of communication delays i.e. $\dot{E}_{ref} = 0$. Hence, by taking the time derivative of (47) would yield us to:

$$\dot{e}_k^E(t) = \dot{E}_k(t) \qquad (48)$$

By combining (43b) and (48) would give us:

$$\frac{dv_k^E}{dt} = K_E \left[\sum_{l=1}^n b_{kl} \left(e_l^E(t-\tau) - e_k^E(t) \right) - \Omega_k \left(e_k^E(t) \right) \right] \qquad (49)$$

To derive the stability conditions for delay independent system, a Lyapunov function for (49) can be given as:

$$V_E(t) = \sum_{k=1}^n \left(e_k^E(t) \right)^2 + \sum_{k=1}^n \sum_{l=1}^n b_{kl} \int_{t-\tau}^t \left(e_l^E(s) \right)^2 ds \qquad (50)$$

Take the derivative of (50) with respect to time along with (49) would yield us to:

$$\dot{V}_E(t) = 2 \sum_{k=1}^n \sum_{l=1}^n b_{kl} e_k^E(t) \left(e_l^E(t-\tau) - e_k^E(t) \right)$$
$$- 2 \sum_{k=1}^n \Omega_k \left(e_k^E(t) \right)^2 + \sum_{k=1}^n \sum_{l=1}^n b_{kl}$$
$$\times \left(\left(e_l^E(t) \right)^2 - \left(e_l^E(t-\tau) \right)^2 \right) \qquad (51)$$

As the communication graph is balanced, thus:

$$\sum_{k=1}^n \sum_{l=1}^n b_{kl} \left(e_k^E(t) \right)^2 = \sum_{k=1}^n \sum_{l=1}^n b_{kl} \left(e_l^E(t) \right)^2 \qquad (52)$$

Apply (52) in (51) would give us:

$$\dot{V}_E(t) = - \sum_{k=1}^n \sum_{l=1}^n b_{kl} \left(e_k^E(t) - e_l^E(t-\tau) \right)^2$$
$$- 2 \sum_{k=1}^n \Omega_k \left(e_k^E(t) \right)^2 \qquad (53)$$

From (53), it can be observed that $\dot{V}_E(t) < 0$, thus $V_E(t) \to 0$, it means that the voltages of the DGs converges to E_{ref} asymptotically.

APPENDIX C
REACTIVE POWER SHARING CONTROLLER
Consider the dynamics in (45) in vector form for simplicity, thus, it can be written as:

$$\frac{dv_k^Q}{dt} = X_Q v(t) + X_{Q-1} v(t - \tau(t)) \qquad (54)$$

where, X_Q and X_{Q-1} are constant positive $n \times n$ matrices. Let a Lyapunov function given below as:

$$V_Q(v_t) = v^T(t) G_Q v(t) \tag{55}$$

where, G_Q is positive $n \times n$ matrices i.e. $G_Q > 0$ and are positive definite and symmetric. According to Razumikhin's theorem, when the condition

$$\sigma_Q v^T(t) G_Q v(t) - v^T(t - \tau(t)) G_Q v(t - \tau(t)) \geq 0 \tag{56}$$

holds for some constant $\sigma_Q = 1 + \vartheta_Q$, where, $\vartheta_Q > 0$, it can be concluded that for any $\aleph_Q > 0$, there exists $\beta_Q > 0$ such that:

$$
\begin{aligned}
&\dot{V}_Q(v(t)) \\
&= 2v^T(t) G_Q \left[X_Q v(t) + X_{Q-1} v(t - \tau(t)) \right] \\
&\leq 2v^T(t) G_Q \left[X_Q v(t) + X_{Q-1} v(t - \tau(t)) \right] + \aleph_Q \\
&\quad \left[\sigma_Q v^T(t) G_Q v(t) - v^T(t - \tau(t)) G_Q v(t - \tau(t)) \right] \\
&\leq -\beta_Q |v(t)|^2
\end{aligned}
\tag{57}
$$

if

$$
\begin{bmatrix}
X_Q^T G_Q + G_Q X_Q + \aleph_Q G_Q & G_Q X_{Q-1} \\
X_{Q-1}^T G_Q & -\aleph_Q G_Q
\end{bmatrix} < 0 \tag{58}
$$

REFERENCES

[1] H. Ali, G. Magdy, and D. Xu, "A new optimal robust controller for frequency stability of interconnected hybrid microgrids considering non-inertia sources and uncertainties," *Int. J. Electr. Power Energy Syst.*, vol. 128, Jun. 2021, Art. no. 106651.

[2] S. Som, S. De, S. Chakrabarti, S. R. Sahoo, and A. Ghosh, "A robust controller for battery energy storage system of an islanded AC microgrid," *IEEE Trans. Ind. Informat.*, vol. 18, no. 1, pp. 207–218, Jan. 2022.

[3] C. Wang, B. Cui, and Z. Wang, "Analysis of solvability boundary for droop-controlled microgrids," *IEEE Trans. Power Syst.*, vol. 33, no. 5, pp. 5799–5802, Sep. 2018.

[4] M. Y. A. Khan, H. Liu, R. Zhang, Q. Guo, H. Cai, and L. Huang, "A unified distributed hierarchal control of a microgrid operating in islanded and grid connected modes," *IET Renew. Power Gener.*, vol. 17, no. 10, pp. 2489–2511, 2023.

[5] B. Liu and Y. Feng, "An adaptive-based control law for accurate frequency restoration and economic load dispatch in microgrid with clock drifts," *Energy Rep.*, vol. 8, pp. 1340–1348, Aug. 2022.

[6] M. Y. A. Khan, H. Liu, J. Shang, and J. Wang, "Distributed hierarchal control strategy for multi-bus AC microgrid to achieve seamless synchronization," *Electric Power Syst. Res.*, vol. 214, Jan. 2023, Art. no. 108910.

[7] Q. Zhou, M. Shahidehpour, A. Alabdulwahab, A. Abusorrah, L. Che, and X. Liu, "Cross-layer distributed control strategy for cyber resilient microgrids," *IEEE Trans. Smart Grid*, vol. 12, no. 5, pp. 3705–3717, Sep. 2021.

[8] E. A. Coelho, D. Wu, J. M. Guerrero, J. C. Vasquez, T. Dragicevic, C. Stefanovic, and P. Popovski, "Small-signal analysis of the microgrid secondary control considering a communication time delay," *IEEE Trans. Ind. Electron.*, vol. 63, no. 10, pp. 6257–6269, Oct. 2016.

[9] S. Liu, X. Wang, and P. X. Liu, "Impact of communication delays on secondary frequency control in an islanded microgrid," *IEEE Trans. Ind. Electron.*, vol. 62, no. 4, pp. 2021–2031, Apr. 2015.

[10] M. A. Shahab, B. Mozafari, S. Soleymani, N. M. Dehkordi, H. M. Shourkaei, and J. M. Guerrero, "Stochastic consensus-based control of μGs with communication delays and noises," *IEEE Trans. Power Syst.*, vol. 34, no. 5, pp. 3573–3581, Sep. 2019.

[11] K. Hashmi, M. M. Khan, M. U. Shahid, A. Nawaz, A. Khan, J. Jun, and H. Tang, "An energy sharing scheme based on distributed average value estimations for islanded AC microgrids," *Int. J. Electr. Power Energy Syst.*, vol. 116, Mar. 2020, Art. no. 105587.

[12] J. Lai, H. Zhou, X. Lu, X. Yu, and W. Hu, "Droop-based distributed cooperative control for microgrids with time-varying delays," *IEEE Trans. Smart Grid*, vol. 7, no. 4, pp. 1775–1789, Jul. 2016.

[13] B. Zhao, X. Dong, and J. Bornemann, "Service restoration for a renewable-powered microgrid in unscheduled island mode," *IEEE Trans. Smart Grid*, vol. 6, no. 3, pp. 1128–1136, May 2015.

[14] B. Ning, Q.-L. Han, and L. Ding, "Distributed finite-time secondary frequency and voltage control for islanded microgrids with communication delays and switching topologies," *IEEE Trans. Cybern.*, vol. 51, no. 8, pp. 3988–3999, Aug. 2021.

[15] Z. Yi, Y. Xu, W. Gu, and Z. Fei, "Distributed model predictive control based secondary frequency regulation for a microgrid with massive distributed resources," *IEEE Trans. Sustain. Energy*, vol. 12, no. 2, pp. 1078–1089, Apr. 2021.

[16] Y. Shan, J. Hu, K. W. Chan, and S. Islam, "A unified model predictive voltage and current control for microgrids with distributed fuzzy cooperative secondary control," *IEEE Trans. Ind. Informat.*, vol. 17, no. 12, pp. 8024–8034, Dec. 2021.

[17] F. Wang, B. Chen, X. Lin, and C. Lin, "Finite-time adaptive fuzzy tracking control design for nonlinear systems," *IEEE Trans. Fuzzy Syst.*, vol. 26, no. 3, pp. 1207–1216, Jun. 2018.

[18] M. Raeispour, H. Atrianfar, H. R. Baghaee, and G. B. Gharehpetian, "Resilient H_∞ consensus-based control of autonomous AC microgrids with uncertain time-delayed communications," *IEEE Trans. Smart Grid*, vol. 11, no. 5, pp. 3871–3884, Sep. 2020.

[19] W. Yao, Y. Wang, Y. Xu, C. Deng, and Q. Wu, "Distributed weight-average-prediction control and stability analysis for an islanded microgrid with communication time delay," *IEEE Trans. Power Syst.*, vol. 37, no. 1, pp. 330–342, Jan. 2022.

[20] W. Yao, Y. Wang, Y. Xu, and C. Dong, "Small-signal stability analysis and lead-lag compensation control for DC networked-microgrid under multiple time delays," *IEEE Trans. Power Syst.*, vol. 38, no. 1, pp. 921–933, Jan. 2023.

[21] Y. Xie and Z. Lin, "Distributed event-triggered secondary voltage control for microgrids with time delay," *IEEE Trans. Syst., Man, Cybern., Syst.*, vol. 49, no. 8, pp. 1582–1591, Aug. 2019.

[22] S. Ullah, L. Khan, I. Sami, and N. Ullah, "Consensus-based delay-tolerant distributed secondary control strategy for droop controlled AC microgrids," *IEEE Access*, vol. 9, pp. 6033–6049, 2021.

[23] W. Hu, Z. Wu, X. Lv, and V. Dinavahi, "Robust secondary frequency control for virtual synchronous machine-based microgrid cluster using equivalent modeling," *IEEE Trans. Smart Grid*, vol. 12, no. 4, pp. 2879–2889, Jul. 2021.

[24] P. Cai, C. Wen, and C. Song, "Consensus-based secondary frequency control for islanded microgrid with communication delays," in *Proc. Int. Conf. Control, Autom. Inf. Sci. (ICCAIS)*, Oct. 2018, pp. 107–112.

[25] X. Lu, N. Chen, Y. Wang, L. Qu, and J. Lai, "Distributed impulsive control for islanded microgrids with variable communication delays," *IET Control Theory Appl.*, vol. 10, no. 14, pp. 1732–1739, Sep. 2016.

[26] X. Wu, Y. Xu, J. He, C. Shen, G. Chen, J. C. Vasquez, and J. M. Guerrero, "Delay-dependent small-signal stability analysis and compensation method for distributed secondary control of microgrids," *IEEE Access*, vol. 7, pp. 170919–170935, 2019.

[27] W. Zhang, W. Liu, T. Wang, A. Liu, Z. Zeng, H. Song, and S. Zhang, "Adaption resizing communication buffer to maximize lifetime and reduce delay for WVSNs," *IEEE Access*, vol. 7, pp. 48266–48287, 2019.

[28] C. Godsil and G. F. Royle, *Algebraic Graph Theory*. Berlin, Germany: Springer, 2001.

[29] J. Schiffer, R. Ortega, A. Astolfi, J. Raisch, and T. Sezi, "Conditions for stability of droop-controlled inverter-based microgrids," *Automatica*, vol. 50, no. 10, pp. 2457–2469, Oct. 2014.

[30] P. Kundur, "Power system stability," in *Power System Stability and Control*, vol. 10, 2007, pp. 1–7.

[31] F. Guo, C. Wen, J. Mao, and Y.-D. Song, "Distributed secondary voltage and frequency restoration control of droop-controlled inverter-based microgrids," *IEEE Trans. Ind. Electron.*, vol. 62, no. 7, pp. 4355–4364, Jul. 2015.

[32] M. Y. Ali Khan, H. Liu, Z. Yang, and X. Yuan, "A comprehensive review on grid connected photovoltaic inverters, their modulation techniques, and control strategies," *Energies*, vol. 13, no. 16, p. 4185, Aug. 2020.

[33] M. Y. A. Khan, H. Liu, S. Habib, D. Khan, and X. Yuan, "Design and performance evaluation of a step-up DC–DC converter with dual loop controllers for two stages grid connected PV inverter," *Sustainability*, vol. 14, no. 2, p. 811, Jan. 2022.

[34] M. Abadi and S. M. Sadeghzadeh, "A control approach with seamless transition capability for a single-phase inverter operating in a microgrid," *Int. J. Electr. Power Energy Syst.*, vol. 111, pp. 475–485, Oct. 2019.

[35] F. Gao and M. R. Iravani, "A control strategy for a distributed generation unit in grid-connected and autonomous modes of operation," *IEEE Trans. Power Del.*, vol. 23, no. 2, pp. 850–859, Apr. 2008.

[36] Z. Kan, Z. Guo, C. Zhang, and X. Meng, "Research on droop control of inverter interface in autonomous microgrid," in *Proc. Int. Power Electron. Appl. Conf. Expo.*, Nov. 2014, pp. 195–199.

[37] J. W. Simpson-Porco, Q. Shafiee, F. Dörfler, J. C. Vasquez, J. M. Guerrero, and F. Bullo, "Secondary frequency and voltage control of islanded microgrids via distributed averaging," *IEEE Trans. Ind. Electron.*, vol. 62, no. 11, pp. 7025–7038, Nov. 2015.

[38] S. Pankaj, J. S. Kumar, and R. K. Nema, "Comparative analysis of MIT rule and Lyapunov rule in model reference adaptive control scheme," *Innov. Syst. Des. Eng.*, vol. 2, no. 4, pp. 154–162, 2011.

[39] K. Gu, J. Chen, and V. L. Kharitonov, *Stability of Time-Delay Systems*. Berlin, Germany: Springer, 2003.

[40] E. Fridman, "Tutorial on Lyapunov-based methods for time-delay systems," *Eur. J. Control*, vol. 20, no. 6, pp. 271–283, Nov. 2014.

[41] W. Michiels and S. Niculescu, *Stability and Stabilization of Time-Delay Systems: An Eigenvalue-Based Approach*. Philadelphia, PA, USA: SIAM," 2007.

[42] F. Milano, "Small-signal stability analysis of large power systems with inclusion of multiple delays," *IEEE Trans. Power Syst.*, vol. 31, no. 4, pp. 3257–3266, Jul. 2016.

[43] W. Sun, Z. Fang, L. Huang, Q. Li, W. Li, and X. Xu, "Distributed robust secondary control of islanded microgrid with stochastic time-varying delays and external disturbances," *Int. J. Electr. Power Energy Syst.*, vol. 143, Dec. 2022, Art. no. 108448.

[44] S. Kim, K.-J. Park, and C. Lu, "A survey on network security for cyber–physical systems: From threats to resilient design," *IEEE Commun. Surveys Tuts.*, vol. 24, no. 3, pp. 1534–1573, 3rd Quart., 2022.

XINGHUA HUANG received the M.S. degree in electrical engineering and automation from Xi'an Jiaotong University, China, in 2018.

He is currently a member of the State Grid Fujian Electric Power Research Institute and Fujian Key Enterprise Laboratory of High Reliability for Power Distribution Technology. His research interests include the operation control of distributed generation and regional electric power grid dispatch.

YUANLIANG FAN received the Ph.D. degree in electrical engineering and automation from Zhejiang University, China, in 2015.

He is currently a Senior Expert with State Grid Fujian Electric Power Company Ltd. His research interests include the operation control of distributed generations, microgrids, and distribution Internet of Things.

HAN WU received the M.S. degree in electrical engineering and automation from Fuzhou University, China, in 2011.

He is currently a Chairman of the State Grid Fujian Electric Power Research Institute Distribution Center. His research interests include distribution Internet of Things and distribution automation.

GONGLIN ZHANG received the M.S. degree in electrical engineering and automation from Fuzhou University, China, in 2010.

He has rich work experience in distribution automation and distribution network operation control. His research interests include distribution automation and operation control of distributed generations.

ZILI YIN received the M.S. degree in electrical engineering and automation from North China Electric Power University, China, in 2007.

He is currently a Chief of the Power Control Center, State Grid Fujian Electric Power Company Ltd., and a professor level Senior Engineer. His research interests include distribution network scheduling control and operation control of distributed generations.

MUHAMMAD YASIR ALI KHAN received the Ph.D. degree in electrical engineering from Hohai University, China, in 2023, where he is currently pursuing the Postdoctoral degree.

His research interests include power electronics converters and microgrid control.

HAOMING LIU (Senior Member, IEEE) received the B.S., M.S., and Ph.D. degrees from Nanjing University of Science and Technology, China, in 1998, 2001, and 2003, respectively.

He is currently a Full Professor with the School of Electrical and Power Engineering, Hohai University. His research interests include new energy generation, distribution system analysis and control, and electricity market.

JINGJING ZHAI received the Ph.D. degree in control engineering from Nanjing University of Science and Technology, Nanjing, China, in 2022.

Currently, she is a Senior Laboratory Technician with Nanjing Institute of Technology. Her research interests include integrated energy system optimal operation and smart power utilization.

● ● ●